

Quantification of extra-cerebral and cerebral hemoglobin concentrations during physical exercise using time-domain near infrared spectroscopy

HÉLOÏSE AUGER,^{1,2} LOUIS BHERER,^{3,4} ÉTIENNE BOUCHER,²
RICHARD HOGE,^{3,5} FRÉDÉRIC LESAGE,^{1,6} AND MATHIEU
DEHAES^{1,2,7,*}

¹Institute of Biomedical Engineering, Université de Montréal, Montréal, QC, Canada

²Centre Hospitalier Universitaire Sainte-Justine, Montréal, QC, Canada

³Institut Universitaire de Gériatrie de Montréal, Montréal, QC, Canada

⁴PERFORM Centre, Concordia University, Montréal, QC, Canada

⁵Department of Neurology and Neurosurgery, McGill University, Montréal, QC, Canada

⁶Department of Electrical Engineering, École Polytechnique de Montréal, Montréal, QC, Canada

⁷Department of Radiology, Radio-oncology and Nuclear Medicine, Université de Montréal, Montréal, QC, Canada

*mathieu.dehaes@umontreal.ca

Abstract: Fitness is known to have beneficial effects on brain anatomy and function. However, the understanding of mechanisms underlying immediate and long-term neurophysiological changes due to exercise is currently incomplete due to the lack of tools to investigate brain function during physical activity. In this study, we used time-domain near infrared spectroscopy (TD-NIRS) to quantify and discriminate extra-cerebral and cerebral hemoglobin concentrations and oxygen saturation (SO_2) in young adults at rest and during incremental intensity exercise. In extra-cerebral tissue, an increase in deoxy-hemoglobin (HbR) and a decrease in SO_2 were observed while only cerebral HbR increased at high intensity exercise. Results in extra-cerebral tissue are consistent with thermoregulatory mechanisms to dissipate excess heat through skin blood flow, while cerebral changes are in agreement with cerebral blood flow (CBF) redistribution mechanisms to meet oxygen demand in activated regions during exercise. No significant difference was observed in oxy- (HbO_2) and total hemoglobin (HbT). In addition HbO_2 , HbR and HbT increased with subject's peak power output (equivalent to the maximum oxygen volume consumption; VO_2 peak) supporting previous observations of increased total mass of red blood cells in trained individuals. Our results also revealed known gender differences with higher hemoglobin in men. Our approach in quantifying both extra-cerebral and cerebral absolute hemoglobin during exercise may help to better interpret past and future continuous-wave NIRS studies that are prone to extra-cerebral contamination and allow a better understanding of acute cerebral changes due to physical exercise.

© 2016 Optical Society of America

OCIS codes: (300.6500) Spectroscopy, time-resolved; (170.0110) Imaging systems; (170.1470) Blood or tissue constituent monitoring.

References and links

1. G. Wagner, M. Herbsleb, F. de la Cruz, A. Schumann, F. Br  nner, C. Schachtzabel, A. Gussew, C. Puta, S. Smesny, H. W. Gabriel, J. R. Reichenbach, and K.-J. B  r, "Hippocampal structure, metabolism, and inflammatory response after a 6-week intense aerobic exercise in healthy young adults: a controlled trial." *J. Cereb. Blood Flow Metab.* **35**, 1570–1578 (2015).
2. N. J. Kirk-Sanchez and E. L. McGough, "Physical exercise and cognitive performance in the elderly: current perspectives." *Clin. Interv. Aging* **9**, 51–62 (2014).
3. L. Bherer, K. I. Erickson, and T. Liu-Ambrose, "A Review of the Effects of Physical Activity and Exercise on Cognitive and Brain Functions in Older Adults," *J. Aging. Res.* **2013**, 1–8 (2013).

4. K. I. Erickson, R. L. Leckie, and A. M. Weinstein, "Physical activity, fitness, and gray matter volume." *Neurobiol. Aging* **35 Suppl 2**, S20–S28 (2014).
5. A. M. Weinstein, M. W. Voss, R. S. Prakash, L. Chaddock, A. Szabo, S. M. White, T. R. Wojcicki, E. Mailley, E. McAuley, A. F. Kramer, and K. I. Erickson, "The association between aerobic fitness and executive function is mediated by prefrontal cortex volume," *Brain Behav. Immun.* **26**, 811–819 (2012).
6. K. Ide and N. H. Secher, "Cerebral blood flow and metabolism during exercise." *Prog. Neurobiol.* **61**, 397–414 (2000).
7. M. H. Laughlin, M. J. Davis, N. H. Secher, J. J. van Lieshout, A. A. Arce-Esquivel, G. H. Simmons, S. B. Bender, J. Padilla, R. J. Bache, D. Merkus, and D. J. Duncker, "Peripheral circulation." *Compr. Physiol.* **2**, 321–447 (2012).
8. G. Hellström, W. Fischer-Colbrie, N. G. Wahlgren, and T. Jogestrand, "Carotid artery blood flow and middle cerebral artery blood flow velocity during physical exercise." *J. Appl. Physiol.* **81**, 413–418 (1996).
9. V. Bolduc, N. Thorin-Trescases, and E. Thorin, "Endothelium-dependent control of cerebrovascular functions through age: exercise for healthy cerebrovascular aging." *Am. J. Physiol. Heart Circ. Physiol.* **305**, H620–33 (2013).
10. I. Heinonen, K. K. Kalliokoski, J. C. Hannukainen, D. J. Duncker, P. Nuutila, and J. Knuuti, "Organ-specific physiological responses to acute physical exercise and long-term training in humans." *Physiology (Bethesda)* **29**, 421–436 (2014).
11. J. González-Alonso, M. K. Dalsgaard, T. Osada, S. Volianitis, E. A. Dawson, C. C. Yoshiga, and N. H. Secher, "Brain and central haemodynamics and oxygenation during maximal exercise in humans." *J. Physiol. (Lond.)* **557**, 331–342 (2004).
12. T. D. Noakes, "Maximal oxygen uptake: "classical" versus "contemporary" viewpoints: a rebuttal." *Med. Sci. Sports Exerc.* **30**, 1381–1398 (1998).
13. H. Boecker and A. Drzezga, "A perspective on the future role of brain pet imaging in exercise science." *Neuroimage* **131**, 73–80 (2016).
14. C. R. Rooks, N. J. Thom, K. K. McCully, and R. K. Dishman, "Effects of incremental exercise on cerebral oxygenation measured by near-infrared spectroscopy: a systematic review." *Prog. Neurobiol.* **92**, 134–150 (2010).
15. F. F. Jöbsis, "Noninvasive, infrared monitoring of cerebral and myocardial oxygen sufficiency and circulatory parameters." *Science* **198**, 1264–1267 (1977).
16. A. W. Subudhi, A. C. Dimmen, and R. C. Roach, "Effects of acute hypoxia on cerebral and muscle oxygenation during incremental exercise." *J. Appl. Physiol.* **103**, 177–183 (2007).
17. T. Rupp, R. Thomas, S. Perrey, and P. Stephane, "Prefrontal cortex oxygenation and neuromuscular responses to exhaustive exercise." *Eur. J. Appl. Physiol.* **102**, 153–163 (2008).
18. C. H. E. Imray, S. D. Myers, K. T. S. Pattinson, A. R. Bradwell, C. W. Chan, S. Harris, P. Collins, and A. D. Wright, "Effect of exercise on cerebral perfusion in humans at high altitude." *J. Appl. Physiol.* **99**, 699–706 (2005).
19. K. Oussaidene, F. Prieur, S. Tagougui, A. Abaidia, R. Matran, and P. Mucci, "Aerobic fitness influences cerebral oxygenation response to maximal exercise in healthy subjects." *Respir. Physiol. Neurobiol.* **205**, 53–60 (2015).
20. R. Jung, M. Moser, S. Baucsek, S. Dern, and S. Schneider, "Activation patterns of different brain areas during incremental exercise measured by near-infrared spectroscopy." *Exp. Brain Res.* **233**, 1175–1180 (2015).
21. S. Mekari, S. Fraser, L. Bosquet, C. Bonnéry, V. Labelle, P. Pouliot, F. Lesage, and L. Bherer, "The relationship between exercise intensity, cerebral oxygenation and cognitive performance in young adults," *Eur. J. Appl. Physiol.* pp. 1–9 (2015).
22. K. Shibuya, J. Tanaka, N. Kuboyama, S. Murai, and T. Ogaki, "Cerebral cortex activity during supramaximal exhaustive exercise." *J. Sports Med. Phys. Fitness* **44**, 215–219 (2004).
23. K.-I. Shibuya, J. Tanaka, N. Kuboyama, and T. Ogaki, "Cerebral oxygenation during intermittent supramaximal exercise." *Respir. Physiol. Neurobiol.* **140**, 165–172 (2004).
24. G. Ganesan, S. Y. Leu, A. Cerussi, B. Tromberg, D. M. Cooper, and P. Galassetti, "Cerebral and Muscle Tissue Oxygenation During Incremental Cycling in Male Adolescents Measured by Time-Resolved Near-Infrared Spectroscopy," *Pediatr. Exerc. Sci.* **28**, 275–285 (2016).
25. P. Ekekekakis, "Illuminating the black box: investigating prefrontal cortical hemodynamics during exercise with near-infrared spectroscopy." *J. Sport. Exerc. Psychol.* **31**, 505–553 (2009).
26. T. Miyazawa, M. Horiuchi, H. Komine, J. Sugawara, P. J. Fadel, and S. Ogoh, "Skin blood flow influences cerebral oxygenation measured by near-infrared spectroscopy during dynamic exercise," *Eur. J. Appl. Physiol.* **113**, 2841–2848 (2013).
27. L. Gagnon, K. Perdue, D. N. Greve, D. Goldenholz, G. Kaskhedikar, and D. A. Boas, "Improved recovery of the hemodynamic response in diffuse optical imaging using short optode separations and state-space modeling." *Neuroimage* **56**, 1362–1371 (2011).
28. L. Gagnon, M. A. Yücel, D. A. Boas, and R. J. Cooper, "Further improvement in reducing superficial contamination in NIRS using double short separation measurements," *Neuroimage* **85**, 127–135 (2014).
29. R. B. Saager and A. J. Berger, "Direct characterization and removal of interfering absorption trends in two-layer turbid media," *J. Opt. Soc. Am. A* **22**, 1874–1882 (2005).
30. A. T. Eggebrecht, B. R. White, S. L. Ferradal, C. Chen, Y. Zhan, A. Z. Snyder, H. Dehghani, and J. P. Culver, "A quantitative spatial comparison of high-density diffuse optical tomography and fMRI cortical mapping," *Neuroimage* **61**, 1120–1128 (2012).
31. A. Torricelli, D. Contini, A. Pifferi, M. Caffini, R. Re, L. Zucchelli, and L. Spinelli, "Time domain functional NIRS

- imaging for human brain mapping." *Neuroimage* **85 Pt 1**, 28–50 (2014).
32. A. Pifferi, A. Torricelli, P. Taroni, and R. Cubeddu, "Reconstruction of absorber concentrations in a two-layer structure by use of multidistance time-resolved reflectance spectroscopy." *Opt. Lett.* **26**, 1963–1965 (2001).
 33. A. Liebert, H. Wabnitz, J. Steinbrink, H. Obrig, M. Möller, R. Macdonald, A. Villringer, and H. Rinneberg, "Time-resolved multidistance near-infrared spectroscopy of the adult head: intracerebral and extracerebral absorption changes from moments of distribution of times of flight of photons." *Appl. Opt.* **43**, 3037–3047 (2004).
 34. L. Gagnon, C. Gauthier, R. D. Hoge, F. Lesage, J. Selb, and D. A. Boas, "Double-layer estimation of intra- and extracerebral hemoglobin concentration with a time-resolved system." *J. Biomed. Opt.* **13**, 054019 (2008).
 35. S. Ijichi, T. Kusaka, K. Isobe, K. Okubo, K. Kawada, M. Namba, H. Okada, T. Nishida, T. Imai, and S. Itoh, "Developmental changes of optical properties in neonates determined by near-infrared time-resolved spectroscopy." *Pediatr. Res.* **58**, 568–573 (2005).
 36. C. T. Davies and A. J. Sargeant, "Circadian variation in physiological responses to exercise on a stationary bicycle ergometer." *Br. J. Ind. Med.* **32**, 110–114 (1975).
 37. P.-O. Leclerc, "Développement d'un système de spectroscopie infrarouge résolue temporellement pour la quantification des concentrations d'hémoglobine cérébrale," Master's thesis, Institut de Génie Biomédical, Université de Montréal (2011).
 38. D. A. Boas, A. M. Dale, and M. A. Franceschini, "Diffuse optical imaging of brain activation: approaches to optimizing image sensitivity, resolution, and accuracy." *Neuroimage* **23 Suppl 1**, S275–S288 (2004).
 39. M. Diop and K. St Lawrence, "Improving the depth sensitivity of time-resolved measurements by extracting the distribution of times-of-flight." *Biomed. Opt. Express* **4**, 447–459 (2013).
 40. O. Dupuy, C. J. Gauthier, S. A. Fraser, L. Desjardins-Crépeau, M. Desjardins, S. Mekary, F. Lesage, R. D. Hoge, P. Pouliot, and L. Bherer, "Higher levels of cardiovascular fitness are associated with better executive function and prefrontal oxygenation in younger and older women." *Front. Hum. Neurosci.* **9**, 66 (2015).
 41. V. Labelle, L. Bosquet, S. Mekary, and L. Bherer, "Decline in executive control during acute bouts of exercise as a function of exercise intensity and fitness level." *Brain Cogn.* **81**, 10–17 (2013).
 42. A. Kienle, M. S. Patterson, N. Dögnitz, R. Bays, G. Wagnîres, and H. van den Bergh, "Noninvasive determination of the optical properties of two-layered turbid media." *Appl. Opt.* **37**, 779–791 (1998).
 43. D. Contini, A. Torricelli, A. Pifferi, L. Spinelli, F. Paglia, and R. Cubeddu, "Multi-channel time-resolved system for functional near infrared spectroscopy." *Opt. Express* **14**, 5418–5432 (2006).
 44. C. Bonnéry, P.-O. Leclerc, M. Desjardins, R. Hoge, L. Bherer, P. Pouliot, and F. Lesage, "Changes in diffusion path length with old age in diffuse optical tomography." *J. Biomed. Opt.* **17**, 056002 (2012).
 45. R. Wolthuis, M. van Aken, K. Fountas, J. S. Robinson, H. A. Bruining, and G. J. Puppels, "Determination of water concentration in brain tissue by Raman spectroscopy." *Anal. Chem.* **73**, 3915–3920 (2001).
 46. S. Wray, M. Cope, D. T. Delpy, J. S. Wyatt, and E. O. Reynolds, "Characterization of the near infrared absorption spectra of cytochrome aa3 and haemoglobin for the non-invasive monitoring of cerebral oxygenation." *Biochim. Biophys. Acta* **933**, 184–192 (1988).
 47. K. Sato, S. Ogoh, A. Hirasawa, A. Oue, and T. Sadamoto, "The distribution of blood flow in the carotid and vertebral arteries during dynamic exercise in humans," *J. Physiol. (Lond.)* **589**, 2847–2856 (2011).
 48. D. Comelli, A. Bassi, A. Pifferi, P. Taroni, A. Torricelli, R. Cubeddu, F. Martelli, and G. Zaccanti, "In vivo time-resolved reflectance spectroscopy of the human forehead." *Appl. Opt.* **46**, 1717–1725 (2007).
 49. E. Ohmae, Y. Ouchi, M. Oda, T. Suzuki, S. Nobesawa, T. Kanno, E. Yoshikawa, M. Futatsubashi, Y. Ueda, H. Okada, and Y. Yamashita, "Cerebral hemodynamics evaluation by near-infrared time-resolved spectroscopy: correlation with simultaneous positron emission tomography measurements." *Neuroimage* **29**, 697–705 (2006).
 50. O. Pucci, V. Toronov, and K. St Lawrence, "Measurement of the optical properties of a two-layer model of the human head using broadband near-infrared spectroscopy." *Appl. Opt.* **49**, 6324–6332 (2010).
 51. L. Li, S. Mac-Mary, J.-M. Sainthillier, S. Nouveau, O. de Lacharriere, and P. Humbert, "Age-Related Changes of the Cutaneous Microcirculation in vivo," *Gerontology* **52**, 142–153 (2006).
 52. N. Uranova, I. Zimina, O. Vikhreva, V. Rachmanova, A. Klintsova, and D. Orlovskaya, "Reduced Capillary Density in the Prefrontal Cortex in Schizophrenia," *AJMSM* **1**, 45–51 (2013).
 53. A. Timinkul, M. Kato, T. Omori, C. C. Deocaris, A. Ito, T. Kizuka, Y. Sakairi, T. Nishijima, T. Asada, and H. Soya, "Enhancing effect of cerebral blood volume by mild exercise in healthy young men: a near-infrared spectroscopy study." *Neurosci. Res.* **61**, 242–248 (2008).
 54. T. Takahashi, Y. Takikawa, R. Kawagoe, S. Shibuya, T. Iwano, and S. Kitazawa, "Influence of skin blood flow on near-infrared spectroscopy signals measured on the forehead during a verbal fluency task." *Neuroimage* **57**, 991–1002 (2011).
 55. M. Dehaes, L. Gagnon, F. Lesage, M. Pélégri-issac, A. Vignaud, R. Valabrègue, R. Grebe, F. Wallois, and H. Benali, "Quantitative investigation of the effect of the extra-cerebral vasculature in diffuse optical imaging: a simulation study." *Biomed. Opt. Express* **2**, 680–695 (2011).
 56. L. Gagnon, M. A. Yücel, M. Dehaes, R. J. Cooper, K. L. Perdue, J. Selb, T. J. Huppert, R. D. Hoge, and D. A. Boas, "Quantification of the cortical contribution to the NIRS signal over the motor cortex using concurrent NIRS-fMRI measurements." *Neuroimage* **59**, 3933–3940 (2012).
 57. B. Hallacoglu, A. Sassaroli, and S. Fantini, "Optical characterization of two-layered turbid media for non-invasive, absolute oximetry in cerebral and extracerebral tissue." *PLoS ONE* **8**, e64095 (2013).

58. H. Mairbäurl, "Red blood cells in sports: effects of exercise and training on oxygen supply by red blood cells." *Front. Physiol.* **4**, 332 (2013).
59. W. Schmidt and N. Prommer, "Impact of alterations in total hemoglobin mass on VO₂max." *Exerc. Sport Sci. Rev.* **38**, 68–75 (2010).
60. T. Li, Q. Luo, and H. Gong, "Gender-specific hemodynamics in prefrontal cortex during a verbal working memory task by near-infrared spectroscopy." *Behav. Brain Res.* **209**, 148–153 (2010).
61. M. Kameyama, M. Fukuda, T. Uehara, and M. Mikuni, "Sex and age dependencies of cerebral blood volume changes during cognitive activation: a multichannel near-infrared spectroscopy study." *Neuroimage* **22**, 1715–1721 (2004).
62. N. Jausovec and K. Jausovec, "Do women see things differently than men do?" *Neuroimage* **45**, 198–207 (2009).
63. W. G. Murphy, "The sex difference in haemoglobin levels in adults — Mechanisms, causes, and consequences," *Blood Rev.* **28**, 41–47 (2014).
64. C. C. Sherwood, A. D. Gordon, J. S. Allen, K. A. Phillips, J. M. Erwin, P. R. Hof, and W. D. Hopkins, "Aging of the cerebral cortex differs between humans and chimpanzees." *Proc. Natl. Acad. Sci. USA* **108**, 13029–13034 (2011).
65. H. N. Mayrovitz and M. B. Regan, "Gender differences in facial skin blood perfusion during basal and heated conditions determined by laser Doppler flowmetry." *Microvasc. Res.* **45**, 211–218 (1993).
66. H. Lu, F. Xu, K. M. Rodrigue, K. M. Kennedy, Y. Cheng, B. Flicker, A. C. Hebrank, J. Uh, and D. C. Park, "Alterations in cerebral metabolic rate and blood supply across the adult lifespan." *Cereb. Cortex* **21**, 1426–1434 (2011).
67. K. Ide, F. Pott, J. J. Van Lieshout, and N. H. Secher, "Middle cerebral artery blood velocity depends on cardiac output during exercise with a large muscle mass." *Acta Physiol. Scand.* **162**, 13–20 (1998).
68. J. Pearson, D. A. Low, E. Stöhr, K. Kalsi, L. Ali, H. Barker, and J. González-Alonso, "Hemodynamic responses to heat stress in the resting and exercising human leg: insight into the effect of temperature on skeletal muscle blood flow." *Am. J. Physiol. Regul. Integr. Comp. Physiol.* **300**, R663–73 (2011).
69. I. Vogiatzis, Z. Louvaris, H. Habazettl, D. Athanasopoulos, V. Andrianopoulos, E. Cherouveim, H. Wagner, C. Rousos, P. D. Wagner, and S. Zakynthinos, "Frontal cerebral cortex blood flow, oxygen delivery and oxygenation during normoxic and hypoxic exercise in athletes." *J. Physiol. (Lond.)* **589**, 4027–4039 (2011).

1. Introduction

Regular physical exercise is known to promote brain health. Changes in physical activity and exercise are associated with functional and structural alterations in the brain [1]. In aging populations, exercise-based programs show potential to reduce risk of age-related cognitive decline and neurodegenerative diseases (see these current reviews [2,3]). In particular, brain volume losses associated with decline are attenuated by higher cardiorespiratory fitness [4]. Structural changes mostly occur in brain areas supporting executive functions, such as the prefrontal cortex [5] and are associated with changes in cerebral blood flow (*CBF*) and metabolism [6]. Given current demographic changes, the understanding of mechanisms underlying immediate and long-term neurophysiological changes due to physical exercise is critical.

Cardiovascular and ventilatory responses to acute exercise result in the increase of the amount of blood pumped by the heart (cardiac output), thus raising oxygen level and blood flow to supply mainly cardiac and skeletal muscles [7], but also to regulate the temperature and dissipate excess heat through the skin (thermoregulatory mechanism) [8]. In the brain, regional increases in *CBF* are modest, occur from rest to moderate-to-high intensity exercise and reach a plateau with increasing intensity while global *CBF* shows no change in response to exercise [6]. Increased metabolic demands due to exercise are met by redistributing oxygen supply in active brain regions from areas that are not necessarily solicited during exercise [9,10]. At very high or maximal intensities, oxygenation decline is observed and likely due to decreased regional *CBF* combined with increased cerebral oxygen uptake [11]. This oxygen supply/demand mismatch occurring at maximal intensities is at the origin of the "central governor" hypothesis, which suggests that physical activity is controlled by complex processes to protect vital organs such as the brain and the heart from ischemia [12]. There is no consensus about this theory and additional studies are needed to better understand neurophysiological changes during acute exercise.

Functional magnetic resonance imaging (MRI) is the gold standard for functional brain imaging but is impractical in the study of immediate effects of incremental exercise in realistic settings due to motion artifacts. Positron emission tomography provides quantitative measures of cerebral blood flow and metabolism but necessitates radioactive injection contrast and high costs while

having similar constraints to study exercise [13]. In contrast, near infrared spectroscopy (NIRS) is a non-invasive, non-ionizing, low-cost and portable imaging technique allowing the study of brain hemodynamics in realistic human research exercise settings (see this systematic review [14]). Continuous-wave NIRS (CW-NIRS) systems allow to retrieve changes in relative oxy- (HbO_2) and deoxygenated (HbR) hemoglobin concentrations induced by neuronal activity [15]. These techniques have been used during incremental intensity exercise [14, 16–25]. However, CW-NIRS techniques (1) provide relative rather than absolute measurements and (2) are known to be strongly contaminated by extra-cerebral signals as hemoglobin changes were retrieved with a simple homogeneous head model. This contamination may even be amplified by the hemoglobin changes occurring in the skin vasculature that are associated with the performance of physical exercise [26]. While recent studies proposed the use of short distance optical channels [27–29] or high-density optical configurations [30] to better discriminate extra-cerebral changes in the measured signals, conventional CW-NIRS techniques remain limited to detect relative changes.

In contrast to CW-NIRS, time-domain NIRS (TD-NIRS), also known as time-resolved spectroscopy, has the ability to quantify absolute tissue optical properties, namely the absorption and scattering coefficients (see this recent review of functional studies in the human brain [31]). Using time-correlated single photon counting, the measure of time of flight of photons to differentiate changes in optical properties at different depths of tissue is possible [32–34]. Using a multiple source-detector distances approach, absolute estimates of the optical parameters are obtained and absolute hemoglobin concentrations are retrieved. Thus, hemoglobin oxygen saturation (SO_2) can be calculated by the ratio of HbO_2 and total hemoglobin (HbT), where HbT is the sum of HbO_2 and HbR , and is proportional to cerebral blood volume (CBV) [35]. When combined with a two-layer representation of the human head, this approach allows to isolate hemoglobin concentrations in the brain and prevent its contamination by extra-cerebral tissue.

In this study, we propose to use a multi-wavelength and multi-distance TD-NIRS approach combined with a two-layer data fitting analysis head model to discriminate and quantify absolute extra-cerebral and cerebral hemoglobin concentrations during incremental physical exercise. To the best of our knowledge, this is the first study to apply this approach to assess hemoglobin changes due to exercise. This quantification may help to better interpret past and future NIRS studies and allow a better understanding of immediate vascular and neuronal changes due to physical exercise.

2. Materials and methods

2.1. Subjects

Ten (10) healthy women and 8 healthy men aged from 18 to 30 years old (mean 23.1 years, SD 2.4 years) were recruited between August 2015 and January 2016 (see Table 1). Average height was 169.6 cm (SD 7.9 cm) and average weight was 62.7 kg (SD 7.6 kg). Exclusion criteria included history of mental or physical pathology, involuntary movements or shaking, epilepsy, smoking, and recent drug or alcohol addiction. Subjects were asked to stop alcohol and caffeine consumption at least 12 hours before testing, and to practice no intense exercise the day before data acquisition. Prior to the study, written consent was obtained from all subjects who also completed a physical activity readiness questionnaire. This study was approved by the Research Ethics Board of the Réseau de Neuroimagerie du Québec (CMER-RNQ), Canada.

2.2. Study protocol

The study protocol included two experimental sessions occurring on two separate days. The first session included the assessment of physical condition and the performance of the maximum oxygen volume consumption test (VO_{2max} , $\text{ml O}_2 \text{ min}^{-1} \text{ kg}^{-1}$) that was used to quantify exercise intensity levels prior to data acquisition [36]. Subjects were first asked to provide a self-evaluation

Table 1. Demographics, physiological and exercise parameters in subjects.

Subject ID	Gender	Age [year]	Height [cm]	Weight [kg]	Init P [W]	PPO [W]
1	W	18	159	57.9	75	142.5
3	W	23	174	64.9	75	195
4	M	24	181	70.9	175	313.75
5	W	25	164.5	53.5	50	185
6	M	21	175	66.2	75	213.75
7	M	24	166	62.5	100	178.75
8	W	24	163.5	57.4	75	150
9	M	24	181.8	65.2	175	265
10	M	27	171.2	71.6	115	253.75
12	W	26	167.2	64.3	75	187.5
14	W	25	168	52.0	35	125
15	W	23	172	55.0	50	181.25
16	W	21	175	63.5	50	203.75
17	M	21	173	79.2	80	260
18	W	21	152	56.0	35	155
Mean (SD)	—	23.1 (2.4)	169.6 (7.9)	62.7 (7.6)	82.7 (43.5)	200.7 (52.5)
Mean (SD)	—	23.5 (2.3)	174.7 (6.0)	69.3 (6.0)	120.0 (44.9)	247.5 (46.4)
Mean (SD)	—	23.0 (2.6)	166.1 (7.4)	58.3 (4.8)	57.8 (17.3)	169.4 (27.0)
M vs. W	—	n.s.	$p = 0.04$	$p < 0.01$	$p < 0.01$	$p < 0.01$

W, women; M, men; Init P, initial power; PPO, peak power output; SD, standard deviation; n.s., non-significant.

of their fitness level in terms of exercise frequency and intensity. The frequency and level of activity as well as the weight and gender of the subjects were then used to determine the initial power to perform the $VO_{2\max}$ test. An ergonomic stationary bicycle allowing subjects to cycle at a constant power measured in watts (W) was used to determine $VO_{2\max}$ (or VO_2 peak) and its corresponding power (W). Until voluntary exhaustion, subjects pedaled continuously during 1-minute levels, each level providing an increment of 15 W in resistance. Thus, the number of levels was equal to the number of minutes pedaled. Oxygen consumption (VO_2) was analyzed throughout the test. The peak power output (PPO) for each subject was determined by the power indicated by the ergonomic bicycle for the last completed level, or adjusted with the proportion of the last incomplete level (see Table 1). While $VO_{2\max}$ was not available for subjects 13 to 18 due to a technical problem with the device, corresponding PPO values were recorded on the bicycle at voluntary exhaustion for all subjects.

The second session consisted in acquiring TD-NIRS data in subjects at rest and while performing exercise at specific intensity levels. Intensity levels were determined as 40% and 80% of the PPO of each subject. Data acquisition was then performed when subjects were cycling at a constant power representing 40% and 80% of their individual PPO.

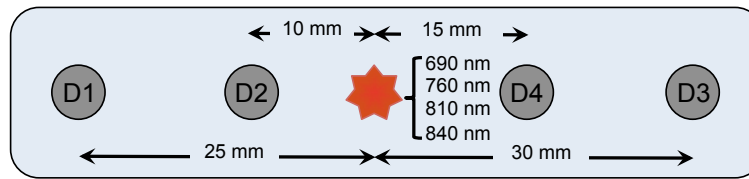


Fig. 1. Schematic representation of the TD-NIRS probe. A fiber coupler light guide was centered and light was emitted at 690, 760, 810 and 840 nm. Four single photon counting avalanche photodiodes (D1 to D4) were placed at 10, 15, 25 and 30 mm.

2.3. TD-NIRS system

The system was custom built in our institution and its development was described elsewhere [37]. Four pulsed lasers (PicoQuant, Berlin, Germany) with wavelengths at 690, 760, 810 and 840 nm were used to emit light. Wavelengths were sufficiently separated by several nm allowing a reduction of random and systematic errors as well as cross-talk [38]. A fiber coupler allowed to bundle all wavelengths in a single optical fiber (see Fig. 1). Four detector optical fibers separated from the laser source by 10, 15, 25 and 30 mm were connected to four single photon counting avalanche photodiodes (SPAD). For each participant, laser intensities were adjusted to avoid optical saturation of the detectors and to maintain counts in the single-photon counting regime.

The TD-NIRS system was accompanied with a specific device to measure the instrument response function (IRF) of each detector. Measuring the IRF allowed to characterize each detector as they have individual response function. The IRF device was made from a series of neutral density filters with optical density of 1.5 and 3. The filters were stacked in a small cylindrical container equipped with connectors on each side.

2.4. Data acquisition

Prior to data acquisition in human, we performed an extensive series of experiments in phantoms with known optical properties to characterize the TD-NIRS system and its IRFs. Experiments were performed in both homogeneous and two-layered phantoms with the same source-detector configuration. Short distance measurements (10 mm) were carefully analyzed to limit the effect of the IRF [39] on estimates of absorption and scattering obtained from this measure.

During data acquisition, the source and detector fibers were maintained in a headband that was positioned on the subject's frontal midline (based on electroencephalography (EEG) 10-20 system) with Velcro straps. The prefrontal cortex was selected as the region of study as it was previously associated with cardiorespiratory fitness as the region responsible for mediating neurophysiological responses to executive function [5,40]. In addition, the absence of hair in frontal skin area reduced potential signal interference between the optical probe and the skin contact. A perforated rubber cap was positioned on the subject's head to cover optical fibers during data acquisition and to optimize the contact between the fibers and the forehead without inducing painful pressure. This cap also served to reduce noise from the ambient light while maintaining the optical probe over the prefrontal cortex during exercise. Windows were obscured and data were acquired in a darkened room.

Data were first acquired at rest and then at 40% and 80% of PPO intensity level, respectively. Half of the subjects followed a "Rest – 40% – 80%" pattern, while the other half followed a "Rest – 80% – 40%" pattern [41]. All subjects were specifically asked to control and limit their head movement while cycling to avoid motion artifacts.

Data acquisition blocks had a duration of 10 min each with an extra 2-min warm-up for 40% and 80% intensity levels. Each block was separated by a 15-min period where the subject was able to rest. During this period, the optical probe was removed to acquire the IRF for all detectors.

To ensure IRF data quality, photon count was maintained within time-correlated single photon counting mode by adjusting the laser diodes alignment to the illumination fiber. The IRF device was positioned between the source fiber and each separate detector fiber, and remained connected for a 1-min data acquisition. A total of three IRF data acquisitions were performed, i.e. after rest, 40% and 80% intensity level data acquisitions, respectively.

Prior to data analysis, datasets acquired for all exercise conditions were inspected for motion artifacts. This systematic review was performed for all source-detector distances and laser sources, i.e. for 16 datasets per condition. Data from subject 2, 11 and 13 were excluded for poor quality data due to an inadequate contact between the optical probe and the subject's forehead or head movement while cycling. Data analysis was then performed with a total of $n_{\text{total}} = 15$ subjects including $n_{\text{women}} = 9$ women and $n_{\text{men}} = 6$ men (see demographics in Table 1).

2.5. Data analysis

Hemoglobin concentrations were estimated with optical properties recovered using a two-layer fitting model [42]. Optical properties are retrieved by modeling the optical fluence φ of each layer such that

$$\varphi_1(z, s) = \frac{\sinh[\alpha_1(z_b + z_0)]}{D_1\alpha_1} \times \frac{D_1\alpha_1 \cosh[\alpha_1(\ell - z)] + D_2\alpha_2 \sinh[\alpha_1(\ell - z)]}{D_1\alpha_1 \cosh[\alpha_1(\ell + z_b)] + D_2\alpha_2 \sinh[\alpha_1(\ell + z_b)]} - \frac{\sinh[\alpha_1(z_0 - z)]}{D_1\alpha_1}, \quad 0 \leq z < z_0 \quad (1)$$

$$\varphi_2(z, s) = \frac{\sinh[\alpha_1(z_b + z_0)] \exp[\alpha_2(\ell - z)]}{D_1\alpha_1 \cosh[\alpha_1(\ell + z_b)] + D_2\alpha_2 \sinh[\alpha_1(\ell + z_b)]}, \quad z > z_0 \quad (2)$$

where α_i and D_i are describing the optical properties of the layer i for $i = \{1, 2\}$, while z_b , z_0 and ℓ are describing the geometry and boundary of the medium (see [42] for precise details). The absorption coefficient (μ_a , cm^{-1}), scattering coefficient (μ_s , cm^{-1}) and an amplitude factor were recovered by fitting the theoretical temporal point spread function (TPSF) with the experimental TPSF at each wavelength λ and for each distance, leading to 16 TPSF fits [34]. Prior to fitting the data, theoretical TPSF were convolved with corresponding IRF to avoid the introduction of a time-dependent parameter in the fitting procedure. These 16 convolved TPSF were first fitted using a homogeneous model [34, 43] to provide initial values of the optical properties, which were injected into the two-layer model. In the two-layer model, the first layer (defined as the extra-cerebral tissue) included the scalp, skull and cerebrospinal fluid while the second layer (defined as the cerebral tissue) included the grey and white matter. The thickness of the extra-cerebral layer was fixed to 13 mm (range 8.75–16 mm, SD 2.1 mm) for men and 14 mm (range 10.75–18 mm, SD 2.0 mm) for women as MRI anatomical measurements were not available for each subject. These values were calculated from the average of MRI thickness measures in 15 men (age 26 ± 2 years) and 12 women (age 25 ± 2 years), respectively reported in our previous studies [37, 44]. The thickness of the cerebral layer was considered semi-infinite.

Quantification of absolute hemoglobin concentrations was performed with retrieved values of μ_a from the two-layer model. Cerebral tissue were assumed to be composed of a fixed 78% of water concentration (H_2O) proportion [45]. Assuming known extinction coefficients (ξ) from literature [46], concentrations of HbO_2 and HbR [$\mu \text{ mol/l}$] were calculated by inverting the linear system:

$$\begin{bmatrix} \mu_a(\lambda_1) \\ \mu_a(\lambda_2) \\ \mu_a(\lambda_3) \\ \mu_a(\lambda_4) \end{bmatrix} = \begin{bmatrix} \xi_{HbO_2}(\lambda_1) & \xi_{HbR}(\lambda_1) & \xi_{H_2O}(\lambda_1) \\ \xi_{HbO_2}(\lambda_2) & \xi_{HbR}(\lambda_2) & \xi_{H_2O}(\lambda_2) \\ \xi_{HbO_2}(\lambda_3) & \xi_{HbR}(\lambda_3) & \xi_{H_2O}(\lambda_3) \\ \xi_{HbO_2}(\lambda_4) & \xi_{HbR}(\lambda_4) & \xi_{H_2O}(\lambda_4) \end{bmatrix} \begin{bmatrix} HbO_2 \\ HbR \\ H_2O \end{bmatrix} \quad (3)$$

HbO_2 and HbR were then used to derive SO_2 and HbT as described above.

2.6. Statistical analysis

Primary statistical analysis was performed to compare absolute values of extra-cerebral and cerebral HbO_2 , HbR , HbT and SO_2 acquired during 40% PPO, 80% PPO, and rest using general linear mixed models. Each comparison was performed with a fixed intercept and compound symmetric covariance matrix. In a second analysis, hemoglobin concentrations were correlated to demographic parameters (age, height and weight) and PPO with Pearson correlation statistics. A third analysis was performed to compare hemoglobin concentrations in men and women. All analyses were performed with a significance level at 0.05 and p -values were given for two-sided tests.

3. Results

3.1. Demographics

Mean initial power for all subjects ($n_{\text{total}} = 15$) was 82.7 W (SD 43.5) and ranged between 35 and 175 W while mean PPO was 220.7 W (SD 52.5). Men and women subgroups were not significantly different in age. Height, weight, initial power and PPO were significantly higher in men compared to women. Details are summarized in Table 1.

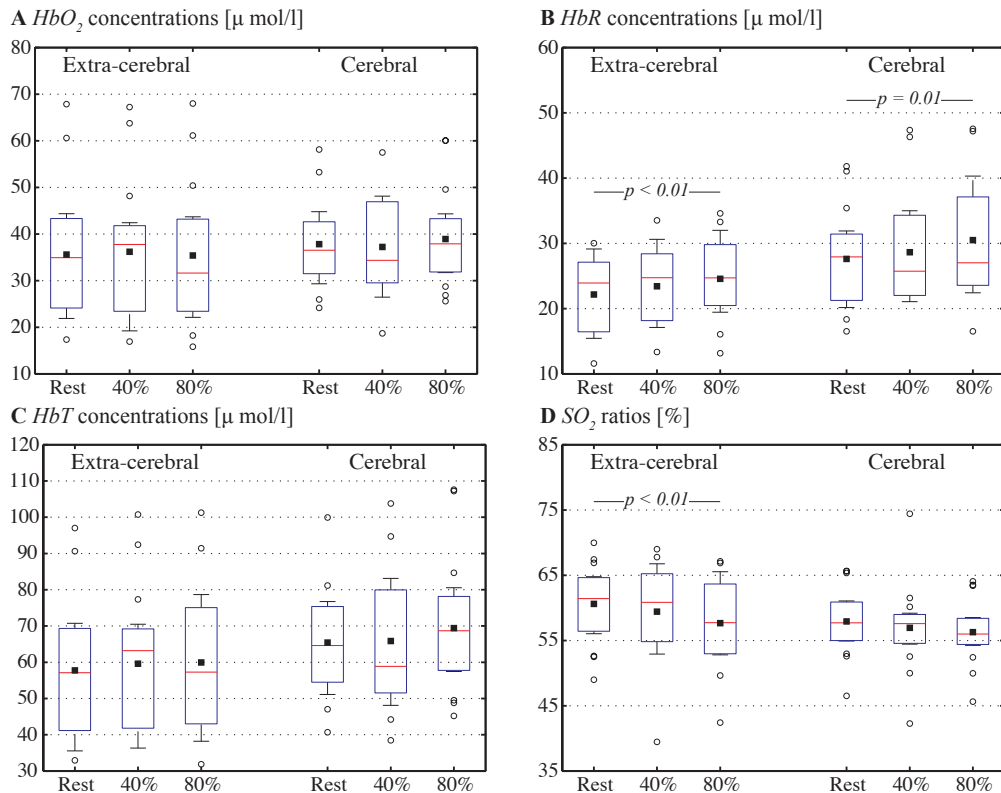


Fig. 2. Boxplots of extra-cerebral and cerebral (A) oxy- (HbO_2), (B) deoxy- (HbR), (C) total hemoglobin (HbT), and (D) hemoglobin oxygen saturation (SO_2) in subjects ($n_{\text{total}} = 15$) at rest, 40% and 80% peak power output (PPO) exercise intensity. On each box, the central mark is the median, the black square is the mean, the edges of the box are the 25th and 75th percentiles, and the whiskers show the standard error of the mean. Empty circles denote outliers and significant statistical comparisons are indicated with their corresponding p -value.

3.2. Comparisons between exercise conditions

Figure 2 shows boxplot distributions of extra-cerebral and cerebral (A) HbO_2 (B) HbR , (C) HbT and (D) SO_2 for all 3 conditions (rest, 40% and 80% intensity levels). Boxplot whiskers represent the standard error of the mean. Subjects at rest had significantly lower extra-cerebral and cerebral HbR compared to values at 80% intensity level of exercise. In contrast, extra-cerebral SO_2 at rest was significantly higher than at 80%. No significant difference was observed in cerebral SO_2 between exercise conditions. None of the comparison between exercise conditions in extra-cerebral and cerebral HbO_2 and HbT was significant.

Table 2. Extra-cerebral vs. cerebral contributions (p -value) in oxy- (HbO_2), deoxy- (HbR), total hemoglobin (HbT) and hemoglobin oxygen saturation (SO_2) values compared at rest, 40% and 80% intensity exercise.

	Rest	40% intensity	80% intensity
HbO_2 [μ mol/l]	n.s.	n.s.	n.s.
HbR [μ mol/l]	$p < 0.01$	$p = 0.01$	$p < 0.01$
HbT [μ mol/l]	$p = 0.03$	$p = 0.02$	$p < 0.01$
SO_2 [%]	n.s.	n.s.	n.s.

n.s., non-significant.

3.3. Comparisons between extra-cerebral and cerebral contributions

Statistical comparisons between extra-cerebral and cerebral hemoglobin concentrations were performed and are provided in Table 2. Both cerebral HbR and cerebral HbT were significantly higher than extra-cerebral values for all exercise conditions (rest, 40% and 80%). Cerebral and extra-cerebral HbO_2 were not significantly different for any condition. While extra-cerebral SO_2 was higher than cerebral values, none of the comparison was significant. In addition, Table 4 (Appendix A) shows statistical comparisons (p -value) of relative changes in hemoglobin concentrations between cerebral and extra-cerebral tissue. Comparisons are provided for relative changes in oxy- (ΔHbO_2), deoxy- (ΔHbR), total hemoglobin (ΔHbT) and hemoglobin oxygen saturation (ΔSO_2). Cerebral ΔHbR during 40% intensity exercise relative to rest was significantly higher than in extra-cerebral tissue. Also, cerebral ΔHbR , ΔHbT and ΔSO_2 during 80% intensity exercise relative to 40% were also significantly higher than in extra-cerebral tissue. None of the comparison was significant for ΔHbO_2 .

Table 3. Relative differences (%) between averaged hemoglobin concentrations (oxy- (HbO_2), deoxy- (HbR) and total hemoglobin (HbT)) recovered with the homogeneous fit and the two-layer fitting model (cerebral layer contribution) for all exercise conditions. p -value is provided for each comparison.

	Rest	40% intensity	80% intensity
HbO_2 [μ mol/l]	10% ($p = 0.02$)	3% (n.s.)	12% ($p < 0.01$)
HbR [μ mol/l]	20% ($p < 0.01$)	18% ($p = 0.02$)	21% ($p < 0.01$)
HbT [μ mol/l]	14% ($p < 0.001$)	9% ($p = 0.01$)	16% ($p < 0.001$)

n.s., non-significant.

Table 3 shows relative differences (%) between averaged hemoglobin concentrations (HbO_2 , HbR and HbT) recovered with the homogeneous model and cerebral values quantified with the

two-layer model, calculated for all exercise conditions. A significant difference was observed for all hemoglobin types and all conditions (only HbO_2 at 40% showed no significant difference). In addition, comparisons between exercise conditions were performed (see Table 5, Appendix A). Significant differences were observed between 80% and rest (HbR , HbT and SO_2), 40% and rest (HbR and HbT) and 80% and 40% (HbR and SO_2). None of the comparison was significant for homogeneous HbO_2 .

3.4. Correlations between hemoglobin, peak power output and demographics

Pearson correlation coefficients (R) with significant p -values are provided in Fig. 3 for relationships between HbO_2 , HbR , and HbT values, and subject's PPO (subject-PPO). All relationships showed an increasing trend between hemoglobin concentrations and subject-PPO. For extra-cerebral contributions (Fig. 3(A)-(C)), HbO_2 and HbT were significantly positively correlated to subject-PPO for all exercise conditions while HbR significantly increased with PPO only at 40% intensity level. For cerebral tissue, HbO_2 and HbT were significantly positively correlated at rest (Fig. 3(D)) while HbR and HbT significantly increased with PPO at 40% intensity level (Fig. 3(E)). None of the correlation was significant between cerebral hemoglobin concentrations and subject-PPO at 80% (Fig. 3(F)). While SO_2 was not significantly correlated with PPO for any condition, SO_2 showed a trend to decrease in the extra-cerebral tissue and remained constant in the cerebral tissue (not shown in Fig. 3).

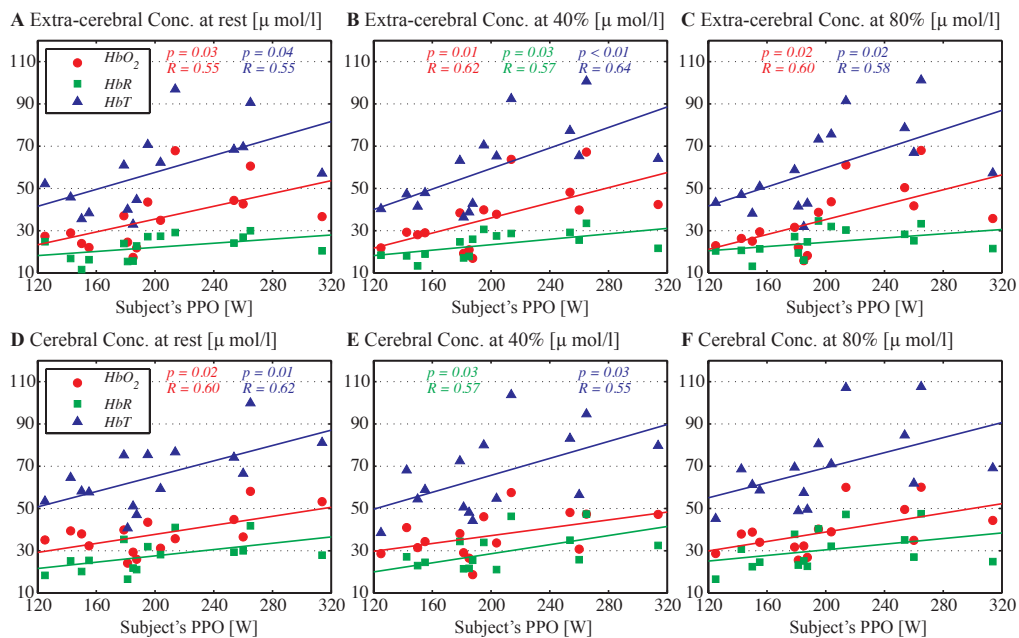


Fig. 3. Pearson correlation coefficients (R) and corresponding p -values between extra-cerebral (A)-(C) and cerebral (D)-(F) hemoglobin concentrations, and subject's peak power output (PPO) at rest, 40% and 80% intensity exercise. Oxy- (HbO_2 , red circles), deoxy- (HbR , green squares) and total hemoglobin (HbT , blue triangles) are displayed with the corresponding linear fits (colored solid lines).

Additional correlations were assessed between hemoglobin concentrations and demographics from Table 1. For extra-cerebral tissue, significant correlations ($p < 0.05$) were found between hemoglobin types (HbO_2 , HbR and HbT) and height and weight for all exercise conditions (only HbR at 80% showed no significance). For cerebral tissue, only three relationships were

significant (HbT with height and weight at rest; HbR with weight at rest). No significant correlation was observed with age for both extra- and cerebral tissue.

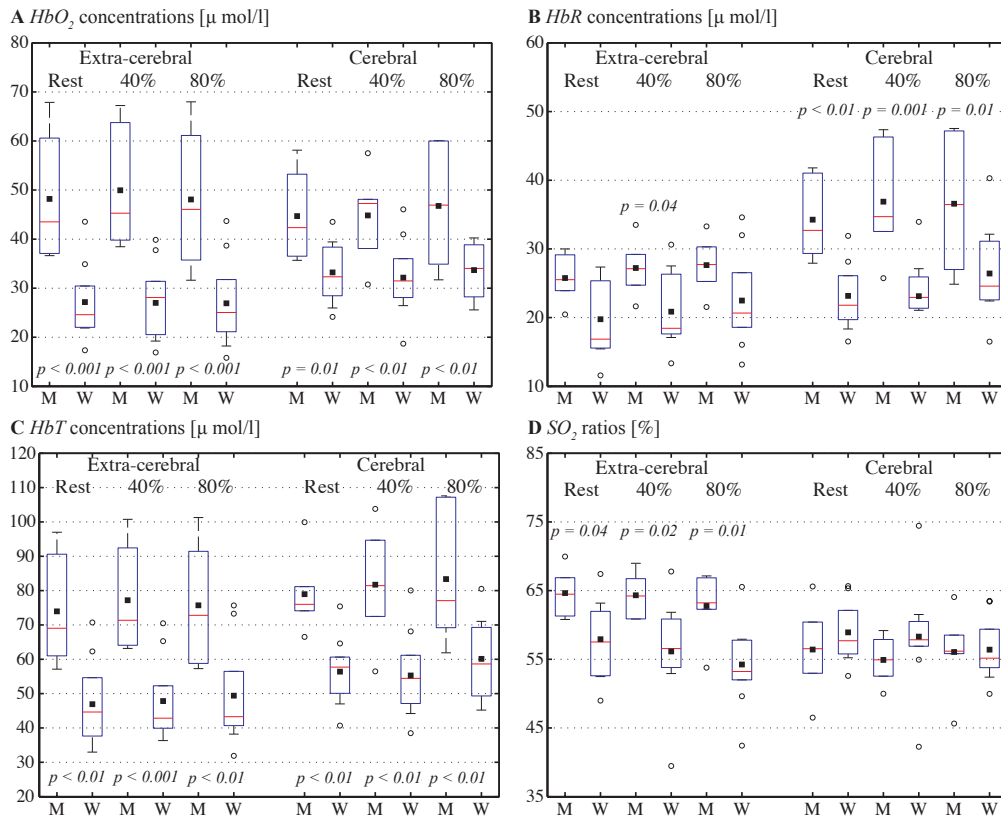


Fig. 4. Boxplots of extra-cerebral and cerebral (A) oxy- (HbO_2), (B) deoxy- (HbR), (C) total hemoglobin (HbT), and (D) hemoglobin oxygen saturation (SO_2) in men (M, $n_{\text{men}} = 6$) and women (W, $n_{\text{women}} = 9$) at rest, 40% and 80% peak power output (PPO) exercise intensity. On each box, the central mark is the median, the black square is the mean, the edges of the box are the 25th and 75th percentiles, and the whiskers show the standard error of the mean. Empty circles denote outliers and significant statistical comparisons are indicated with their corresponding p -value.

3.5. Comparisons between men and women

Figure 4 displays boxplot distributions of extra-cerebral and cerebral hemoglobin concentrations for all conditions when subgrouping subjects by gender (6 men and 9 women). Men (M) had significantly higher HbO_2 , HbR and HbT values compared to women (W) for all conditions. Only extra-cerebral HbR at rest and 80% PPO showed no significance. While extra-cerebral SO_2 was significantly higher in men compared to women for all conditions, cerebral SO_2 was not significantly different between men and women. Results observed in Fig. 2(B) are only confirmed in women with extra-cerebral HbR and SO_2 significantly higher at 80% vs. rest ($p < 0.01$) as well as with cerebral HbR ($p = 0.03$). In addition, cerebral HbR in women was significantly higher at 80% compared to 40% exercise intensity ($p = 0.03$). Statistical comparisons in men were all non-significant.

4. Discussion

In this study, we employed a multi-wavelength and multi-distance TD-NIRS technique with a multi-layer head model to quantify absolute hemoglobin concentrations during incremental physical exercise. This approach allowed us to characterize hemoglobin concentrations in both extra-cerebral and cerebral tissues and demonstrate significantly higher cerebral HbT and HbR compared to extra-cerebral tissue during exercise, and confirmed this observation at rest. Estimated absolute hemoglobin concentrations were significantly different than with the simple homogeneous model and only partly in agreement with previous CW-NIRS studies in exercise, suggesting possible contamination of brain optical properties by extra-cerebral tissue as previously reported at rest. In addition, we confirmed systematic increases in hemoglobin with subject-PPO (equivalent to VO_2 peak) for all exercise conditions, and higher hemoglobin in men compared to women. These observations are consistent with current theories in exercise, will likely help to interpret previous and future NIRS studies and contribute to understanding the origin of the NIRS signal during physical exercise.

4.1. Benefits of the technique

Significant changes observed in extra-cerebral HbR and SO_2 during 80% intensity exercise (Fig. 2) are likely due to increased forehead skin blood flow that is associated with increased blood flow in the external carotid artery during high intensity exercise [47]. These results are in agreement with thermoregulatory vasodilation mechanisms that, among other physiological factors, allow to dissipate excess heat through skin blood flow [8]. This separation of extra-cerebral signals is however not possible with CW-NIRS techniques alone. This limitation is supported by significant differences (up to 21%, Table 3) observed between hemoglobin concentrations recovered with the homogeneous fitting model (reflecting traditional CW-NIRS analysis) and cerebral concentrations estimated with the two-layer model. Furthermore, when comparing hemoglobin concentrations retrieved using the homogeneous model between exercise conditions (Table 5, Appendix A), we confirmed significant changes observed in HbR and SO_2 . Additional comparisons in HbR (40% vs. rest and 80% vs. 40%), HbT (40% and 80% vs. rest) and SO_2 (80% vs. 40%) were significant. These discrepancies are likely due to the contamination of brain optical properties by extra-cerebral tissue when using the homogeneous model [42, 48, 49]. The estimation of hemoglobin concentrations with the homogeneous model may thus be partially biased and not completely reflective of the underlying head physiology. These results emphasize the development of realistic approaches that quantify absolute brain optical properties and limit its contamination by extra-cerebral tissue.

Significantly higher cerebral HbR during high intensity exercise compared to rest (Fig. 2) is consistent with studies that have showed that physical exercise activates executive functions supported by the prefrontal and frontal brain regions (reviewed in [14]). Our results are in agreement with the theory stipulating that the brain has its own control and redistributes local blood flow to meet oxygen demand in cerebral areas that are active from other regions that are not actively solicited during exercise [9, 10]. From the anatomical point of view, the brain is also organized differently than the extra-cerebral tissue with a higher density of blood vessels [51, 52]. Our results also reflect this different vasculature via our measures of HbT , which is proportional to CBV [35]. In particular, we demonstrated that HbT was significantly higher in cerebral compared to extra-cerebral tissue during exercise and confirmed this observation at rest [49]. This agreement in brain function and anatomy during exercise and at rest suggests that our technique allows to quantify brain optical properties and limits their contamination by extra-cerebral tissue.

The effect of incremental exercise on cerebral oxygenation using NIRS instrumentation has been investigated in the last decades (see this systematic meta-data analysis recently published [14]). Despite the inability to discriminate extra-cerebral response, these studies [14, 16–25]

reported hemoglobin changes recovered from signals originated through the whole head. Few of them were performed with a similar experimental design based on incremental intensity levels quantified with individual VO_2 peak or ventilatory thresholds (VT1 and VT2, corresponding to moderate and high intensity exercise, respectively) [16–18, 24]. In particular in Fig. 2, the significant increase in cerebral HbR between 80% and rest was coherent with two studies [16, 17]. Our results in HbO_2 and HbT were also consistent with a CW-NIRS study performed at normal (150 m) altitude [18], while they were not in agreement with significant increases observed between moderate and high exercise intensity compared to rest [16, 17, 24]. In [18], the authors observed significantly higher relative SO_2 (rSO_2) at high intensity compared to rest, which is in the opposite direction of our extra-cerebral SO_2 . Non-significant changes in SO_2 measured with TD-NIRS in Ganesan *et al.* [24] are consistent with our cerebral SO_2 . Furthermore, these studies were also compared with hemoglobin concentrations retrieved using our homogeneous model (Table 5, Appendix A). As for the comparison with the two-layer estimations, significant increases in HbO_2 during incremental exercise [16, 17, 24] were not in agreement with our homogeneous HbO_2 while consistent with [18]. Significant increases in HbR during incremental exercise in [16, 17] were in agreement with our homogeneous HbR . Changes in homogeneous HbT and SO_2 due to exercise were partially in agreement (i.e. not in agreement for all comparisons between exercise conditions) with previous studies [16, 17, 24]. These differences may be due to several factors including the extra-cerebral contamination in NIRS studies performed with the homogeneous analysis and the high variability caused by the heterogeneity in fitness status and gender in our population. Future studies will be conducted with stricter fitness and gender inclusion criteria.

To further show the importance of discriminating cerebral and extra-cerebral contributions, we demonstrated that changes in cerebral HbR during 40% intensity exercise relative to rest were significantly higher than in extra-cerebral tissue (Table 4, Appendix A). In addition, changes in cerebral HbR , HbT and SO_2 during 80% intensity exercise relative to 40% were also significantly higher than in extra-cerebral tissue. These differences suggest that relative changes are also prone to error due to extra-cerebral tissue. Also, the magnitude of our relative changes in the brain was compared qualitatively with previous studies [16, 18, 24, 53] and showed high variability. This variability between these studies is potentially weighted by the extra-cerebral contamination, and therefore the variability would likely decrease by using more accurate models.

Several CW-NIRS studies have reported specific methods to minimize and correct the effect of extra-cerebral tissue. For example, short source-detector separations have been used to model the extra-cerebral contribution that is statistically removed from standard (3 cm) separation measurements [27–29, 54]. Also, the effect of pial vein vasculature on CW-NIRS measurements, which is not related to skin blood flow, has been quantified by Monte Carlo simulations in the occipital cortex [55] and validated with concurrent *in vivo* functional NIRS-MRI measurements in the motor area [56]. While these techniques have shown improvement to model extra-cerebral tissue, they are limited to relative cerebral changes.

Our study opens a perspective in data analysis to correct superficial effects in exercise NIRS studies. Other groups have recently developed NIRS methodologies that allow the absolute quantification of extra-cerebral and cerebral tissue [50, 57], but these techniques have not been applied during exercise. As for our approach, these techniques were based on multi-distance measurements combined with a two-layer head model. While Pucci *et al.* developed a CW-NIRS technique based on a broadband spectral system [50], Hallacoglu *et al.* proposed a frequency-domain NIRS system [57]. In the later study, *in vivo* data acquired in human at rest revealed higher HbT in cerebral compared to extra-cerebral tissue and no difference in SO_2 , which is consistent with our results. In addition, the later method provides the estimation of the individual's scalp-cortex thickness. This approach shows potential for its application in exercise research, as it may allow the reduction of costs associated with subject's MRI examination needed to obtain

individual anatomical measure of the scalp-cortex distance. These studies strongly support the need to routinely measure absolute hemoglobin levels in NIRS and functional NIRS studies.

4.2. *Fitness status and differences in men and women*

Fitness status is known to alter cardiac output, blood flow, oxygen availability and hematocrit in the blood [14, 58, 59]. In trained individuals, a decrease in hematocrit has been observed and associated with an increased plasma volume. This condition is known as “sports anemia” and not well understood. While trained athletes have lower hematocrit (“anemia”), they have an increased total mass of red blood cells and total hemoglobin as compared to untrained subjects. Our results are consistent with these observations as increases in all hemoglobin species with subject-PPO were observed at rest and during exercise (Fig. 3). However, the lack of blood gases analysis providing hematocrit and other physiological parameters limit the extent of our results. Future studies including blood gases analysis and TD-NIRS measures at 100% PPO and higher will allow to better understand sports anemia and the transition to oxygen supply/demand mismatch as well as its effect on cognition.

In this study, we confirmed higher hemoglobin concentrations in men compared to women observed in functional NIRS studies. Frontal changes in cerebral HbO_2 during working memory and word fluency tasks were stronger in men compared to women [60, 61] while frontal cerebral SO_2 at rest and during visual and auditory tasks were also stronger in men [62]. These studies suggest a gender effect in relative hemoglobin changes due to functional stimulation. In contrast to functional studies, our approach provided absolute hemoglobin concentrations. The observed decreases in extra-cerebral and cerebral tissue in women are likely due to a combination of intrinsic physiological factors including a diminished volume (12%) of hemoglobin in the blood (HGB , dl/g) [63], smaller frontal grey matter volumes (20 cc) [64] and a smaller number of perfused microvessels in facial skin [65]. In addition to these factors, our assumption of a fixed scalp-cortex thickness in men and women may also produce up to 15% error for a difference of 1 mm thickness [34]. These factors are likely to account for the differences we observed.

While extra-cerebral SO_2 was significantly higher in men, cerebral SO_2 showed a trend to be slightly higher in women compared to men. In contrast, a multi-distance frequency-domain NIRS study showed higher absolute cerebral SO_2 in male compared to female [62]. The absence of difference we observed would indicate that the amount of available oxygen in the brain is not gender-specific. However, a MRI study recently showed that the cerebral metabolic rate of oxygen consumption ($CMRO_2$) was significantly higher in female compared to male aged from 20 to 90 years old [66]. This lack of consistency in SO_2 indicates the need for additional studies with strict inclusion criteria with respect to gender.

4.3. *Limitations and future studies*

Differences in fitness status and gender represent the main limitation and future studies will be performed with stricter inclusion criteria. Other limitations include data quality affected by head movement during cycling, sweat and cutaneous heat at proximity of the optical probe during data acquisition. Despite these experimental obstacles, subjects were well informed to limit head motion during cycling and our team carefully documented each data acquisition to detect potential source of signal contamination. Careful attention was also made when replacing the optical probe on the subject between data acquisitions. In addition to following the 10-20 EEG system, the replacement was eased by the presence of small and non-painful pressure marks on subjects' forehead. Also, as each subject had specific skin color pigmentation, optical saturation of the detectors had to be adjusted to maintain single photon counting mode. This adjustment is required to ensure statistical robustness when averaging TPSF curves. In addition, additional physiological measurements such as arterial oxygen saturation, heart beat, cardiac output [67], skin temperature [68], Doppler skin blood flow [26] and blood gases (e.g. temperature, HGB ,

lactate, partial pressures) [69] will be monitored in future studies. These additional data will allow to better understand the complex interactions between cerebral and physiological changes during incremental exercise.

We believe our study allows to better interpret CW-NIRS data during exercise and that its results can be used to further analyze past studies as well as future works. Using data collected with our approach on a given population, correction factors could be defined for specific instrumentation and application. As our approach is non-invasive and portable, it also can be used serially in longitudinal study designs such as to assess the effects of exercise-based programs on brain hemoglobin concentrations in aging populations [2]. Our approach can be applied beyond the study of the effects of exercise on hemoglobin concentrations in the brain. For example, it could be applied in the study of cerebral changes in epileptic patients suffering from seizures and interictal epileptic discharges.

5. Conclusion

In summary, we demonstrated extra-cerebral and confirmed cerebral changes in hemoglobin in young healthy subjects during incremental exercise using a TD-NIRS instrumentation with a two-layer head model. Results support previous studies showing the contamination of brain optical properties by extra-cerebral tissue when using simplistic homogeneous model. During high intensity exercise, extra-cerebral changes are likely due to thermoregulatory mechanisms while cerebral changes are consistent with blood flow redistribution mechanisms to meet oxygen demand in activated regions such as the prefrontal cortex supporting executive functions. Increases in hemoglobin concentrations with subject's peak power output (equivalent to VO_2 peak) during incremental exercise is consistent with decreased hematocrit and increased total mass of red blood cells and total hemoglobin observed in trained individuals. In addition, gender differences were observed in absolute hemoglobin concentrations and are consistent with prior studies. Our approach has the potential to improve data interpretation in past and future NIRS studies and may help to better understand neurophysiological mechanisms involved in exercise.

Appendix A

Table 4 reports statistical comparisons (p -value) between extra-cerebral and cerebral relative hemoglobin changes during exercise (40% vs. rest, 80% vs. rest and 80% vs. 40%). Comparisons are given for relative changes in oxy- (ΔHbO_2), deoxy- (ΔHbR), total hemoglobin (ΔHbT) and hemoglobin oxygen saturation (ΔSO_2).

Table 4. Statistical comparisons (p -value) of relative changes in hemoglobin concentrations between cerebral and extra-cerebral tissue. Comparisons are provided for relative changes in oxy- (ΔHbO_2), deoxy- (ΔHbR), total hemoglobin (ΔHbT) and hemoglobin oxygen saturation (ΔSO_2).

	40% vs. Rest	80% vs. Rest	80% vs. 40%
ΔHbO_2 [μ mol/l]	n.s.	n.s.	n.s.
ΔHbR [μ mol/l]	$p = 0.02$	n.s.	$p = 0.048$
ΔHbT [μ mol/l]	n.s.	n.s.	$p = 0.049$
ΔSO_2 [%]	n.s.	n.s.	$p = 0.045$

n.s., non-significant.

Table 5 displays statistical comparisons (p -value) in hemoglobin concentrations retrieved using the homogeneous model between exercise conditions (rest, 40% and 80% intensity levels).

Table 5. Statistical comparisons (p -value) between exercise conditions with hemoglobin concentrations retrieved using the homogeneous model for oxy- (HbO_2), deoxy- (HbR), total hemoglobin (HbT) and hemoglobin oxygen saturation (SO_2) values.

	40% vs. Rest	80% vs. Rest	80% vs. 40%
HbO_2 [μ mol/l]	n.s.	n.s.	n.s.
HbR [μ mol/l]	$p = 0.02$	$p < 0.001$	$p < 0.01$
HbT [μ mol/l]	$p = 0.01$	$p < 0.001$	n.s.
SO_2 [%]	n.s.	$p < 0.01$	$p = 0.01$

n.s., non-significant.

Funding

The authors would like to acknowledge funding from the Natural Sciences and Engineering Research Council of Canada [NSERC 2015-04672 (MD)] and the Fonds de Recherche du Québec – Santé [FRQS 32600 (MD)] as well as scholarship support from the CHU Sainte-Justine (HA) and the Faculty of Graduate and Postdoctoral Studies at Université de Montréal (HA). The content of this article is solely the responsibility of the authors and does not necessarily represent the official views of the funding sources.

Acknowledgments

The authors thank all the participants who consented to perform the study and Francis Compte from the Institut Universitaire de Gériatrie de Montréal who kindly coordinated the study. We also thank Thierry P. Beausoleil and Paul-Olivier Leclerc for their advices and support. Portions of this work were presented as a poster at the OSA Biomedical Optics Congress (session III, paper JW3A.22) in April 2016.

Disclosure/conflict of interest

None to declare.